Lightfield Coordinates Adapted to Asgeirsson's Theorem

Haotian Li, He Qin, Todor Georgiev

Adobe Systems, San Jose, CA 95110, USA

Abstract

John's differential equation and its canonical form, the ultrahyperbolic equation, plays important role in lightfield imaging. The equation describes a local constraint on the lightfield, that was first observed as a "dimensionality gap" [6] in the frequency representation. Related to the ultrahyperbolic equation, Asgeirsson's theorems describe global properties. These indicate new, global, constraints on the lightfield. In order to help validate those theorems on real captured images, we introduce a coordinate system for the lightfield, which suits better the Asgeirsson theorems, and analyze behaviour in terms of the new coordinates.
Keywords: Lightfield, John's equation, ultrahyperbolic PDE, Asgeirsson's theorems, $4D$ radiance.

1 Introduction

1.1 John's Transform and John's Equation

Given a function f describing density of isotropic light sources in $3D$, the John transform r of f is defined as its integral along any straight line ξ:

$$J(f) = r, \qquad r(\xi) := \int_\xi f(x, y, z) \mathrm{d}m(x, y, z), \tag{1}$$

where $\mathrm{d}m$ is the Euclidean measure on the straight lines ξ (notations taken from [5]). If we use two-plane parametrization for ξ (Fig. 1), where (x, y) gives the intersection of a light ray ξ with the first plane and (u, v) indicates the angles by tracking the displacements of ξ on the second plane, then

$$J(f) = r, \qquad r(x, y, u, v) = \int_{-\infty}^{\infty} f(x + uz, y + vz, z) dz \tag{2}$$

John's equation is derived from Eq. (2). It constrains the radiance r in the following way:

$$\left(\frac{\partial}{\partial y}\frac{\partial}{\partial u} - \frac{\partial}{\partial x}\frac{\partial}{\partial v}\right)r = 0 \tag{3}$$
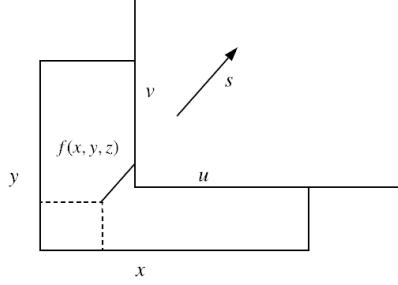
Figure 1: Two parallel planes parameterization of straight lines in $3D$.

1.2 The Ultrahyperbolic Equation

Furthermore, if we do the following reparametrization of $r(x, y, u, v)$ into $\tilde{r}(\xi_1, \xi_2, \xi_3, \xi_4)$ (i.e. transform from $4D$ (x, y, u, v)-space to $4D$ $(\xi_1, \xi_2, \xi_3, \xi_4)$-space),

$$
\begin{cases}
\xi_1 = \frac{1}{2}(u + y) \\
\xi_2 = \frac{1}{2}(u - y) \\
\xi_3 = \frac{1}{2}(v + x) \\
\xi_4 = \frac{1}{2}(v - x)
\end{cases}
\qquad
\begin{cases}
x = \xi_3 - \xi_4 \\
y = \xi_1 - \xi_2 \\
u = \xi_1 + \xi_2 \\
v = \xi_3 + \xi_4
\end{cases}
\tag{4}
$$

we get the ultrahyperbolic partial differential equation

$$
(\partial_{\xi_1 \xi_1} - \partial_{\xi_2 \xi_2} - \partial_{\xi_3 \xi_3} + \partial_{\xi_4 \xi_4})\tilde{r} = 0 \qquad \text{or equivalently, } (\Delta_{14} - \Delta_{23})\tilde{r} = 0, \tag{5}
$$

where Δ_{14} and Δ_{23} are the Laplacians in the (ξ_1, ξ_4) and (ξ_2, ξ_3) planes, respectively. (See [3]).

1.3 Asgeirsson's Theorems

Next we use the ultrahyperbolic equation with four variables as shown in Eq. (5). We base our analysis on the following theorems by Asgeirsson (see [1]).

Theorem 1.1. *Integral over a circle C_1 with radius R in the $(1, 4)$-plane is equal to the integral over the same radius circle C_2 in the $(2, 3)$-plane, i.e.,*

$$
\int_0^{2\pi} r(\xi_1 + R\cos\theta, \xi_2, \xi_3, \xi_4 + R\sin\theta)\mathrm{d}\theta = \int_0^{2\pi} r(\xi_1, \xi_2 + R\cos\theta, \xi_3 + R\sin\theta, \xi_4)\mathrm{d}\theta \tag{6}
$$

Theorem 1.2. *More generally, if we consider a double integral over two circles, one of which has radius R_1 in $(1, 4)$-plane and the other has radius R_2 in $(2, 3)$-plane, it is equal to the double integral over two circles with two radii switched in the two planes, i.e.,*

$$
\int_0^{2\pi} \int_0^{2\pi} r(\xi_1 + R_1\cos\theta_1, \xi_2 + R_2\cos\theta_2, \xi_3 + R_2\sin\theta_2, \xi_4 + R_1\sin\theta_1)\mathrm{d}\theta_1\mathrm{d}\theta_2
$$

$$
= \int_0^{2\pi} \int_0^{2\pi} r(\xi_1 + R_2\cos\theta_1, \xi_2 + R_1\cos\theta_2, \xi_3 + R_1\sin\theta_2, \xi_4 + R_2\sin\theta_1)\mathrm{d}\theta_1\mathrm{d}\theta_2
$$

2

2   New Coordinates

We introduce two sets of polar coordinates in the planes (ξ_1, ξ_4) and (ξ_2, ξ_3), respectively:

$$\begin{cases} \xi_1 = R_1 \cos\theta_1 \\ \xi_4 = R_1 \sin\theta_1 \end{cases} \qquad \begin{cases} \xi_2 = R_2 \cos\theta_2 \\ \xi_3 = R_2 \sin\theta_2 \end{cases} \qquad \text{where } R_1, R_2 \geqslant 0 \text{ and } \theta_1, \theta_2 \in [0, 2\pi).$$

Then, we consider the new coordinate system $(\theta_1, \theta_2, R_1, R_2)$ for the lightfield, in which (θ_1, θ_2) are the coordinates within each new microimage, and (R_1, R_2) are the coordinates of the new microimages. In this coordinate system Theorem 1.2 states that the double integral over (θ_1, θ_2) of a microimage with coordinates (R_1, R_2) is equal to the double integral over (θ_1, θ_2) of a microimage with coordinates (R_2, R_1).

3   Change of Coordinates

Coordinate Transformation: $(\theta_1, \theta_2, R_1, R_2) \longrightarrow (x, y, u, v)$

$$\begin{cases} x = R_2 \sin\theta_2 - R_1 \sin\theta_1 \\ y = R_1 \cos\theta_1 - R_2 \cos\theta_2 \\ u = R_1 \cos\theta_1 + R_2 \cos\theta_2 \\ v = R_2 \sin\theta_2 + R_1 \sin\theta_1 \end{cases} \tag{7}$$

Inverse Coordinate Transformation: $(x, y, u, v) \longrightarrow (\theta_1, \theta_2, R_1, R_2)$

$$\begin{cases} \theta_1 = \arctan2(v - x, u + y) \\ \theta_2 = \arctan2(v + x, u - y) \\ R_1 = \frac{1}{2}\sqrt{(u + y)^2 + (v - x)^2} \\ R_2 = \frac{1}{2}\sqrt{(u - y)^2 + (v + x)^2} \end{cases} \tag{8}$$

where arctan2 is a variation form of arctan (see Fig. 2):

$$\arctan2(y, x) = \begin{cases} \arctan(\frac{y}{x}) & \text{if } x > 0, \\ \arctan(\frac{y}{x}) + \pi & \text{if } x < 0 \text{ and } y \geqslant 0, \\ \arctan(\frac{y}{x}) - \pi & \text{if } x < 0 \text{ and } y < 0, \\ \frac{\pi}{2} & \text{if } x = 0 \text{ and } y > 0, \\ -\frac{\pi}{2} & \text{if } x = 0 \text{ and } y < 0, \\ \text{undefined} & \text{if } x = 0 \text{ and } y = 0. \end{cases} \tag{9}$$

4   Discretization

To deal with real images with pixels, discretization of the previous formulas is necessary. Here we discretize the radii and the angles. First, we simply discretize both radii R_i, $i = 1, 2$, into non-negative integers. For example $R_1 = 0, 1, 2, 3, \cdots$, and similar for R_2. Second, we discretize the
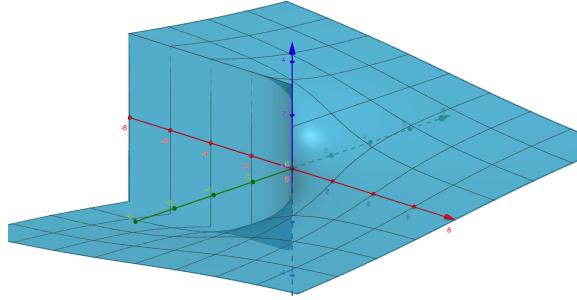
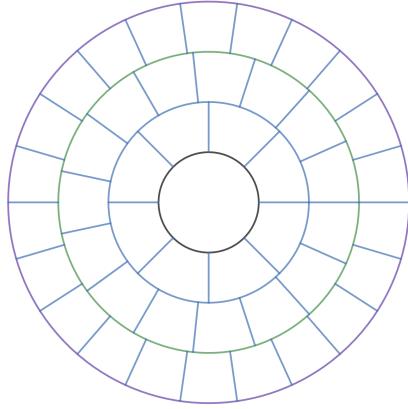Figure 2: Function $z = \arctan 2(y, x)$, x-axis (green), y-axis (blue), z-axis (red)

Figure 3: R_1, θ_1 discretization in plane (ξ_1, ξ_4). The concentric rings represent $R_1 = 0, 1, 2, 3$.

angles θ_i, $i = 1, 2$, in a linear (in R_i) way: For θ_i, we evenly split the interval $[0, 2\pi)$ into $7R_i + 1$ sub-intervals (as shown in Fig. 3). We discretize in a linear fashion in order to produce uniform representation (see below). The Jacobian in polar coordinate is linear w.r.t. the radius value.

After discretization, we arrange the coordinates $(\theta_1, \theta_2, R_1, R_2)$ as shown in Fig. 4. Since pixels are equally spaced, the sizes of different microimages are different. The size of a microimage depends on the number of pixels in it.

Now Asgeirsson's theorems simply say that the sum of all pixels in a microimage with coordinates (R_1, R_2) is equal to the sum of all pixels in the corresponding microimage with coordinates (R_2, R_1). Note that those two microimages are symmetric with respect to the main diagonal in Fig. 4.

5   Numerical Experiments

We use the Seagull lightfield image (Fig. 5) to generate an example of the new lightfield representation (Fig. 6). In the experiments, we choose the pixel at the center of the seagull's eye as the reference point, i.e., the origin of the $4D$ coordinates, in the Seagull lightfield.

Since the coordinate transformation (Eq. (7)) is continuous and analytic, we generally get float-
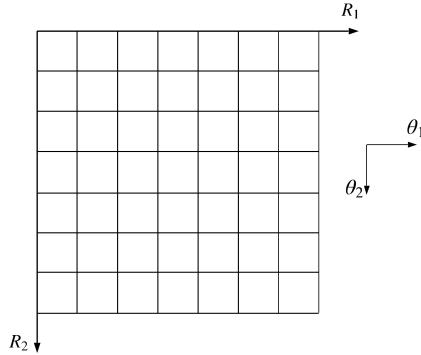
Figure 4: New coordinates for the lightfield. (θ_1, θ_2) are the coordinates of pixels inside each of the small squares / rectangles.

ing point number coordinates instead of integers when we try to fill in the new coordinate system's pixel values. So in Fig. 6, we use nearest neighbor sampling to read the pixel value from the original lightfield image.

Figure 7 is used as a map representing the coordinates in Figure 6.

Figure 8 is a zoom in into Figure 6d, where R_1 and R_2 take values from 0 to 4.

The first Asgeirsson theorem says that the sum of all pixels with given $R_2 = k$ in the single row at the top, is equal to the sum of all pixels in the single column on the left having R_1 equal to the same k.

More generally, the second Asgeirsson theorem says that in symmetric boxes pixels sum up to the same value. Boxes are defined symmetric relative to the main diagonal (see Section 4).

6 Note on Using Shift for Lightfield Imaging

One important practical point about lightfield imaging is sparsity of sampling, and the resulting aliasing. Due to the spatio-angular resolution tradeoff [4] and the need to produce higher spatial resolution with limited sensor size, we often perform sparse optical sampling in the angular dimensions. This results in aliasing artifacts when we render the final image, or when we apply any 4D filter.

This influences our algorithms for rendering of the final image and refocusing. It also influences the computation of derivatives in the angular directions u and v. The same pixel location (x, y) in two neighboring microimages (u, v) and $(u+1, v)$ sample two very different rays in the lightfield and their difference cannot represent correctly the derivative of the radiance in u-direction. This is due to sparse optical sampling. We need a microimage between (u, v) and $(u+1, v)$, which however has not been captured. Considering epipolar geometry, we substitute the pixel with spatial coordinates (x, y) in this missing microimage with a pixel from the $(u+1, v)$ microimage, with shifted x-coordinate. This is the same shift or "patch size" that is used in lightfield/plenoptic rendering (see for example [2]). It depends on depth. For the seagull in our lightfield (Fig. 5) the shift value is 8.78 pixels, which we approximate with 9 in Figures 6, 7, 8.
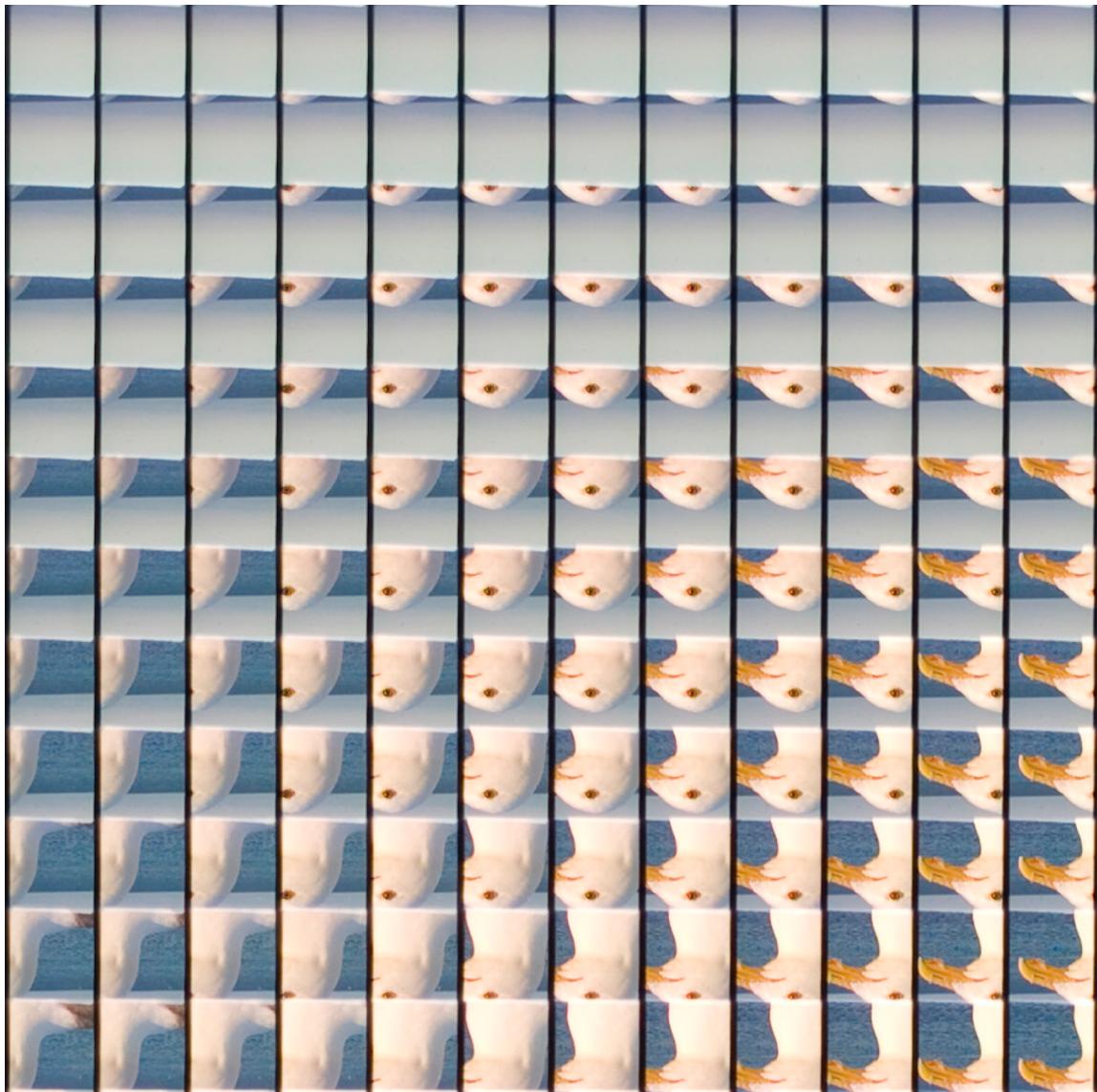
5

Figure 5: Original lightfield Seagull captured with our Plenoptic 2.0 camera. Coordinates are chosen in the traditional way: Microimage locatedion is parametrized by (u, v), pixels microimage having coordinates (x, y).

(a) shift = 0

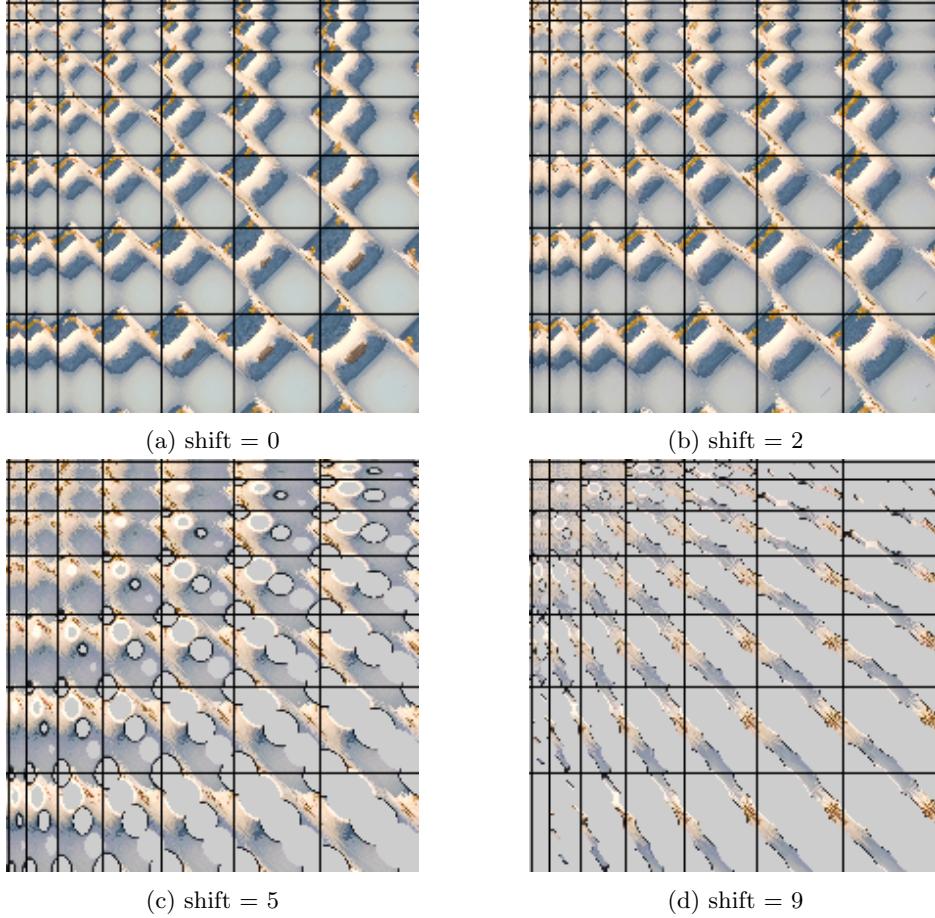(b) shift = 2

(c) shift = 5

(d) shift = 9

Figure 6: New coordinate representations of lightfield Seagull (Fig. 5) with different shifts. The important role of shifts is explained in section 6. See Fig. 7 for colormap and description of our coordinates.

(a) shift = 0

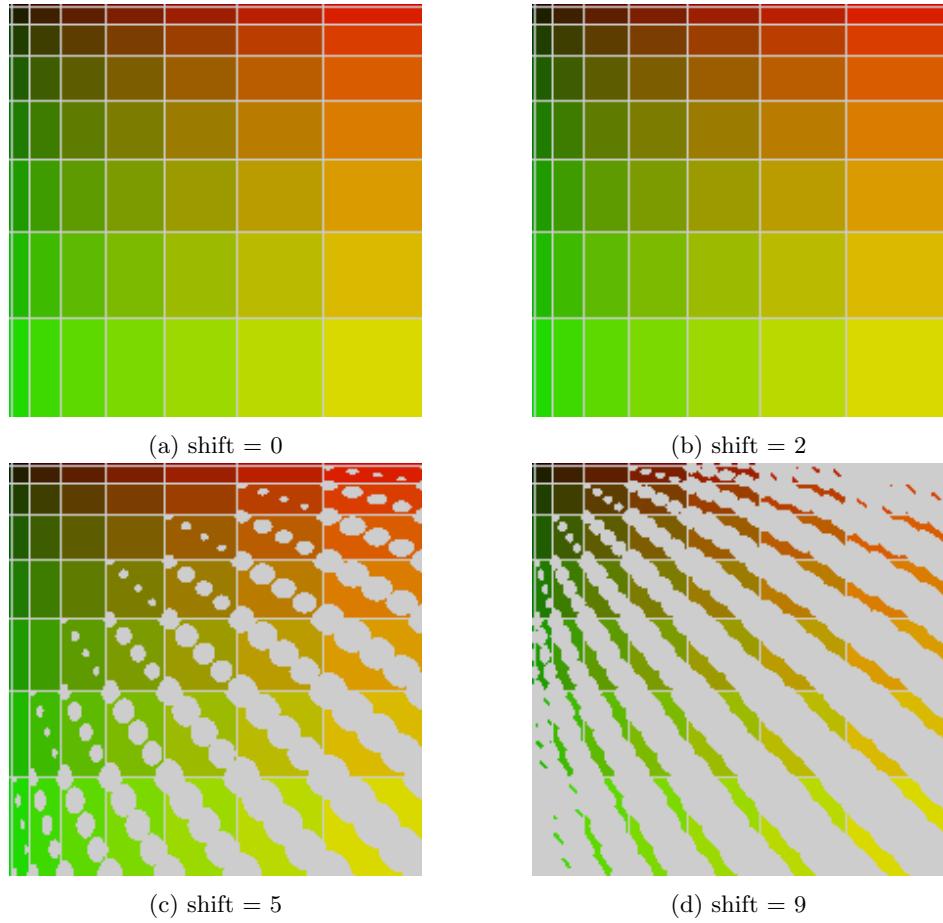(b) shift = 2

(c) shift = 5

(d) shift = 9

Figure 7: Color mapping of the new coordinate representation of lightfield Seagull (Fig. 6) with different shifts. Different tones of green represent values of R_1 from 0 (darkest) to 7 (lightest), and similar for red (representing R_2). Pixels inside each rectangle have coordinates θ_1 and θ_2 ranging from 0 to 2π. Gray represents pixels that are outside the captured lightfield (in our case outside Fig. 5).
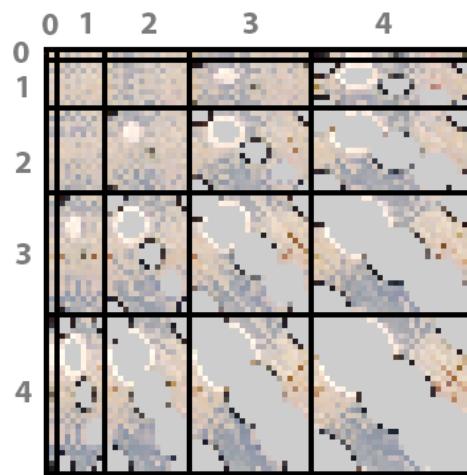
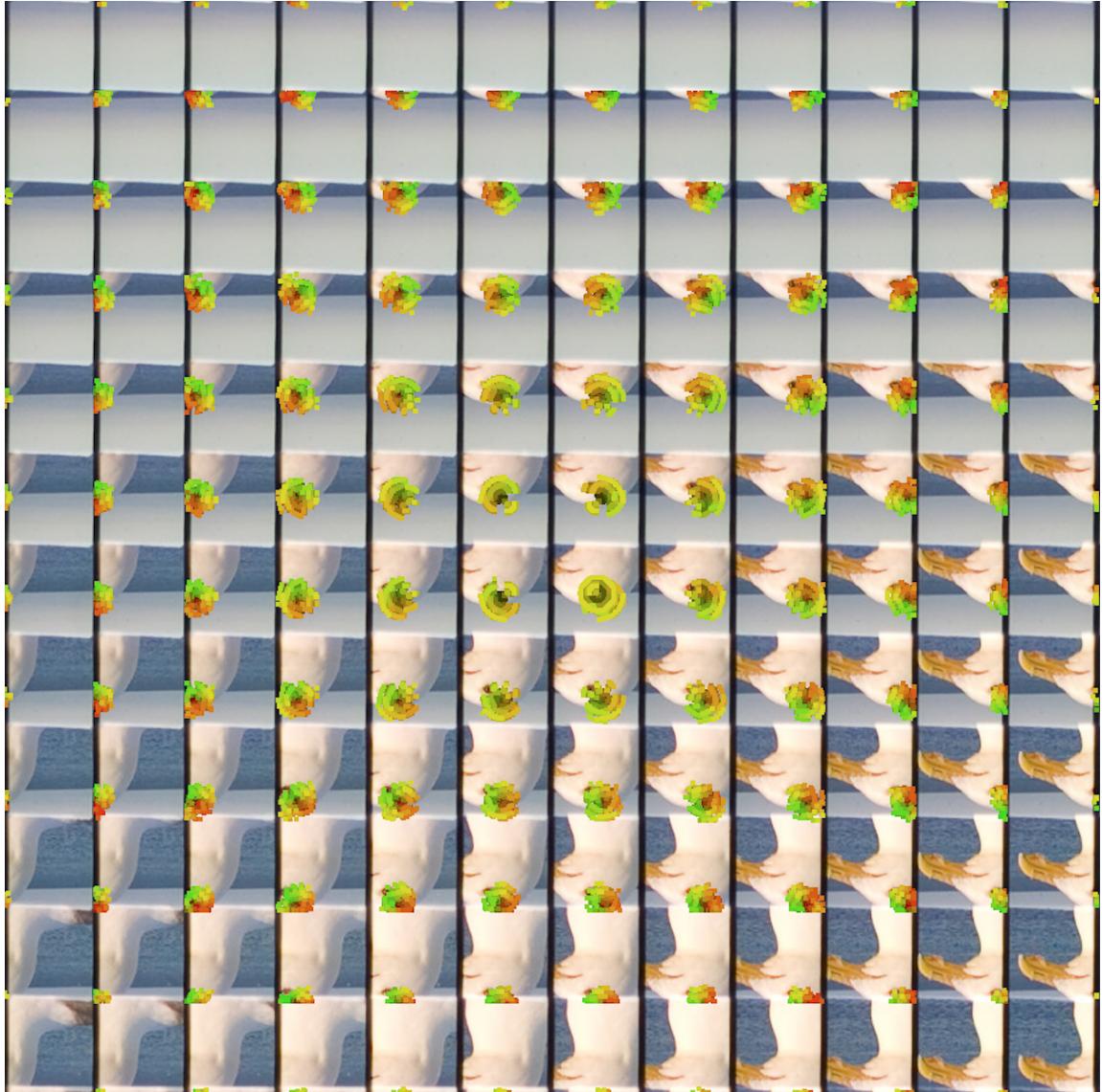Figure 8: A zoom in into Fig. 6d, where R_1 and R_2 take values from 0 to 4.

Figure 9: Color mapping in original coordinates with shift 9.

References

[1] R. Courant and D. Hilbert, *Methods of Mathematical Physics: Partial Differential Equations*, John Wiley & Sons, 2008.

[2] T. Georgiev and A. Lumsdaine, *Focused plenoptic camera and rendering*, Journal of Electronic Imaging, 19 (2010).

[3] T. Georgiev, H. Qin, and H. Li, *John transform and ultrahyperbolic equation for lightfields*, arXiv preprint arXiv:1907.01186, (2019).

[4] T. Georgiev, K. C. Zheng, B. Curless, D. Salesin, S. Nayar, and C. Intwala, *Spatio-angular resolution tradeoff in integral photography*, Proceedings of Eurographics Symposium on Rendering, (2006).

[5] S. Helgason and S. Helgason, *The radon transform*, Springer, 1999.

[6] A. Levin and F. Durand, *Linear view synthesis using a dimensionality gap light field prior*, in 2010 IEEE Computer Society Conference on Computer Vision and Pattern Recognition, June 2010, pp. 1831–1838.